

Functional changes in the structure of the SRP GTPase on binding GDP and Mg²⁺GDP

Douglas M. Freymann¹, Robert J. Keenan², Robert M. Stroud² and Peter Walter^{2,3}

Ffh is a component of a bacterial ribonucleoprotein complex homologous to the signal recognition particle (SRP) of eukaryotes. It comprises three domains that mediate both binding to the hydrophobic signal sequence of the nascent polypeptide and the GTP-dependent interaction of Ffh with a structurally homologous GTPase of the SRP receptor. The X-ray structures of the two-domain 'NG' GTPase of Ffh in complex with Mg²⁺GDP and GDP have been determined at 2.0 Å resolution. The structures explain the low nucleotide affinity of Ffh and locate two regions of structural mobility at opposite sides of the nucleotide-binding site. One of these regions includes highly conserved sequence motifs that presumably contribute to the structural trigger signaling the GTP-bound state. The other includes the highly conserved interface between the N and G domains, and supports the hypothesis that the N domain regulates or signals the nucleotide occupancy of the G domain.

The signal recognition particle (SRP) and the SRP receptor (SR) mediate the co-translational targeting of nascent protein-ribosome complexes to the membrane translocation apparatus¹. The SRP protein subunit (termed Ffh in bacteria) that binds the signal sequence of nascent polypeptides is a GTPase, as is the SR α -subunit (termed FtsY in bacteria)^{2,3}. During targeting, Ffh and FtsY interact directly⁴ and stimulate the GTP hydrolysis activity of each other⁵. In eukaryotic systems GTP binding is sufficient for SRP targeting to the membrane, and GTP hydrolysis is required for subsequent dissociation of the SRP from SR⁶⁻⁸. Ffh is a three-domain protein, comprising a two-domain GTPase (the 'N' and 'G' domains for N-terminal and GTPase domains, respectively) and a C-terminal methionine-rich 'M' domain, which mediates recognition of signal peptide and 4.5S RNA⁹⁻¹¹. The affinity of the SRP GTPase for nucleotide is low relative to other GTPases^{12,13}. Interaction of SRP with ribosome-nascent chain complexes has been shown to increase the affinity of the SRP for GTP¹⁴, while interaction of signal peptides with purified Ffh-FtsY complex inhibits GTPase activity and may stabilize an empty state of the protein^{15,16}.

The crystal structures of the apo-GTPase domains of both Ffh and FtsY have been determined^{17,18}, revealing the common two-domain 'NG' structure unique to the SRP subfamily of GTPases. The G domains of both proteins are structurally homologous to other GTPases, but are distinguished by an extension of the central β -sheet by two additional strands and two α -helices (β 2a- α 1a- β 2b- α 1b; ref. 17), the insertion box domain (IBD; the substructure α 1a- β 2b- α 1b has been termed the I-Box¹³). It contains a highly conserved sequence motif (II; summarized in Fig. 1b) that is unique to the SRP GTPase subfamily and is implicated in the interaction between Ffh and FtsY. In the structure of the apo-NG domain of *Thermus aquaticus* Ffh¹⁷, the side chains of this motif and two other conserved sequence motifs (I and III; Fig. 1b) form a network of hydrogen bond and salt bridge interactions among themselves. This network may serve to stabilize the nucleotide-free state.

The function of the N domain in SRP-SR mediated targeting is unknown. Interaction between the N and M domains of Ffh can be detected in chemical modification and proteolysis experiments^{11,19}, suggesting that one function of the N domain in SRP may be to modulate binding of signal sequences^{11,19-21}. The N domain is tightly associated with the G domain across an interface that is highly conserved in both domains (the 'ALLEADV' motif in N (ref. 21), and the 'DARGG' motif in G (ref. 17)). This interface is adjacent in sequence and structure to the characteristic GTPase motif IV (Fig. 1b) that mediates specificity for the guanine base of the bound nucleotide. In the apo-proteins the spatial arrangement of the GTPase motifs is 'too large' by ~2.5 Å (ref. 18), so that a conformational change must accompany nucleotide binding. This suggests that the interface between the two domains may couple the conformation of the N domain to the GTP-binding site of the G domain, and that consequently the N domain may sense or regulate the nucleotide occupancy state of the GTPase in both SRP and SR.

As a first step toward structural understanding of the mechanism of the GTPase 'switch'²² in this system, we determined the 2.0 Å resolution crystal structures of the NG GTPase of Ffh complexed with Mg²⁺GDP and GDP. The structures provide an explanation for the relatively low affinity of the SRP GTPases for nucleotide and identify two regions of conformational flexibility. These regions may be involved in signaling the active state of the protein and suggest a mechanism by which the N domain modulates the nucleotide-bound state of Ffh.

Structure of the Mg²⁺GDP complex

The structures of the Mg²⁺GDP and GDP complexes of the NG GTPase of Ffh from *T. aquaticus* were determined by molecular replacement (crystallographic statistics are summarized in Table 1). A new structure of the apo form of NG was also determined. We compare four structures in this work, termed A1 (the previous apo structure¹⁷), G1 (GDP), A2 (apo) and G2 (Mg²⁺GDP), that together allow us to assign functional significance to the conformational changes observed on binding to

¹Department of Molecular Pharmacology and Biological Chemistry, Northwestern University Medical School, 303 E. Chicago Avenue, Chicago, Illinois 60611, USA.

²Department of Biochemistry and Biophysics and ³Howard Hughes Medical Institute, University of California, San Francisco, California 94143-0448, USA.

Correspondence should be addressed to D.M.F. email: freymann@nwu.edu

articles

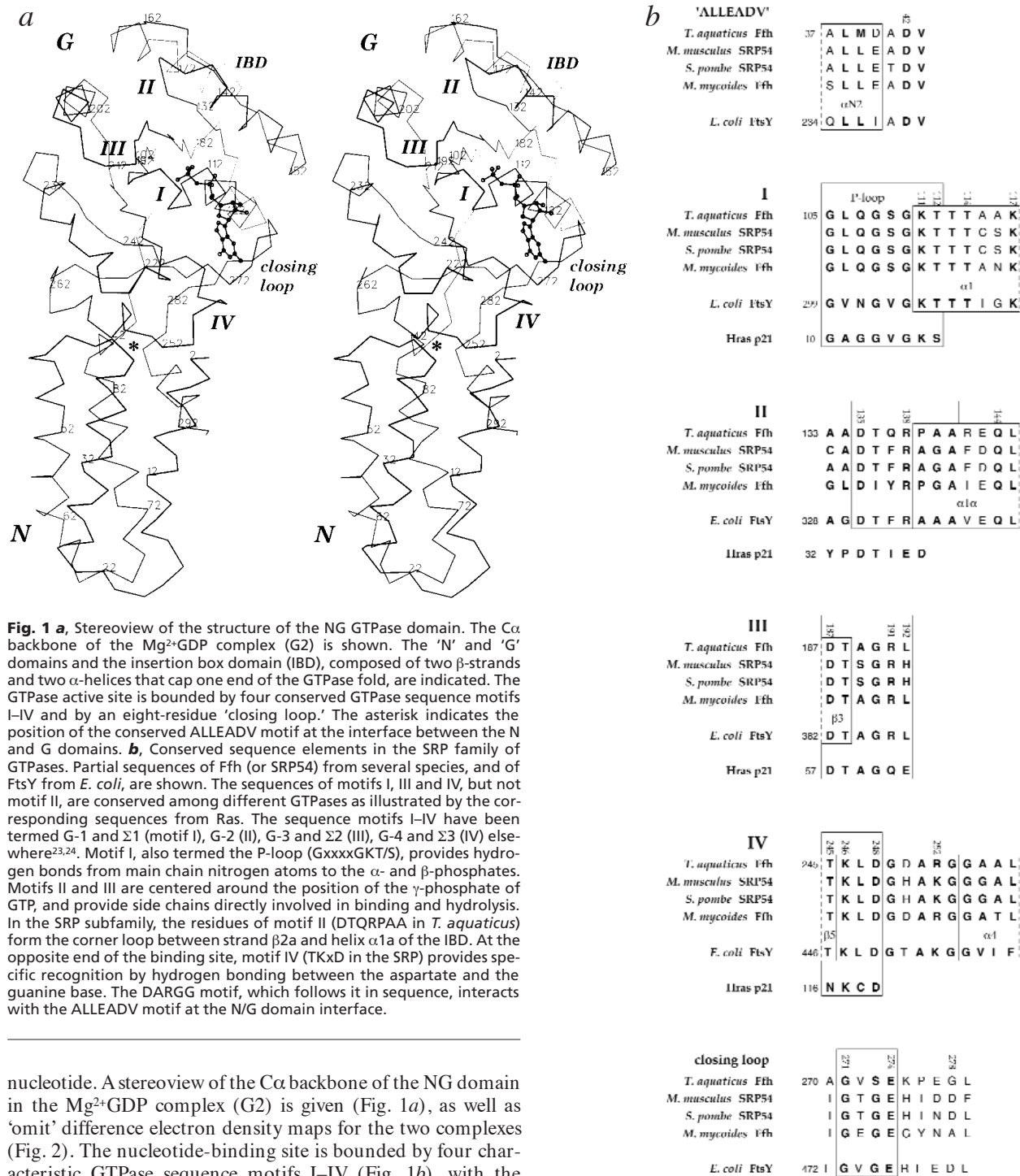


Fig. 1 a, Stereoview of the structure of the NG GTPase domain. The C α backbone of the Mg²⁺GDP complex (G2) is shown. The 'N' and 'G' domains and the insertion box domain (IBD), composed of two β -strands and two α -helices that cap one end of the GTPase fold, are indicated. The GTPase active site is bounded by four conserved GTPase sequence motifs I-IV and by an eight-residue 'closing loop.' The asterisk indicates the position of the conserved ALLEADV motif at the interface between the N and G domains. **b**, Conserved sequence elements in the SRP family of GTPases. Partial sequences of Ffh (or SRP54) from several species, and of FtsY from *E. coli*, are shown. The sequences of motifs I, III and IV, but not motif II, are conserved among different GTPases as illustrated by the corresponding sequences from Ras. The sequence motifs I-IV have been termed G-1 and Σ 1 (motif I), G-2 (II), G-3 and Σ 2 (III), G-4 and Σ 3 (IV) elsewhere^{23,24}. Motif I, also termed the P-loop (GxxxGKT/S), provides hydrogen bonds from main chain nitrogen atoms to the α - and β -phosphates. Motifs II and III are centered around the position of the γ -phosphate of GTP, and provide side chains directly involved in binding and hydrolysis. In the SRP subfamily, the residues of motif II (DTQRPA in *T. aquaticus*) form the corner loop between strand β 2a and helix α 1a of the IBD. At the opposite end of the binding site, motif IV (TKxD in the SRP) provides specific recognition by hydrogen bonding between the aspartate and the guanine base. The DARGG motif, which follows it in sequence, interacts with the ALLEADV motif at the N/G domain interface.

nucleotide. A stereoview of the C α backbone of the NG domain in the Mg²⁺GDP complex (G2) is given (Fig. 1a), as well as 'omit' difference electron density maps for the two complexes (Fig. 2). The nucleotide-binding site is bounded by four characteristic GTPase sequence motifs I-IV (Fig. 1b), with the major specific interactions with the bound nucleoside diphosphate mediated by main chain and side chain atoms of motifs I (the P-loop, residues Gly 105-Thr 112) and IV (residues Thr 245-Asp 248).

Closure around the guanine-binding site

Several features distinguish the interactions of the SRP GTPase with GDP from those seen in the structures of other GDP-bound GTPases. First, opposite motif IV, an additional 'closing loop' packs against the guanine base (Fig. 2). The closing loop comprises eight residues (Gly 271-Gly 278) that are disordered in the first

structure of the apo-NG (A1) and includes a conserved sequence motif in the SRP GTPase subfamily (GxG/SE; Fig. 1b). The side chain of the conserved Glu 274 is at the apex of the loop but is poorly ordered in the structures described here. The position of the closing loop relative to the guanine base is similar to that of a short conserved motif termed Σ 4 (ref. 23) or G-5 (ref. 24) in other GTPases, although it shows no similarity to them in sequence or structure. The loop closes against the nucleotide so that the guanine base is sandwiched by van der Waals interactions between main chain atoms of residues Ser 273 and Glu 274 on one side,

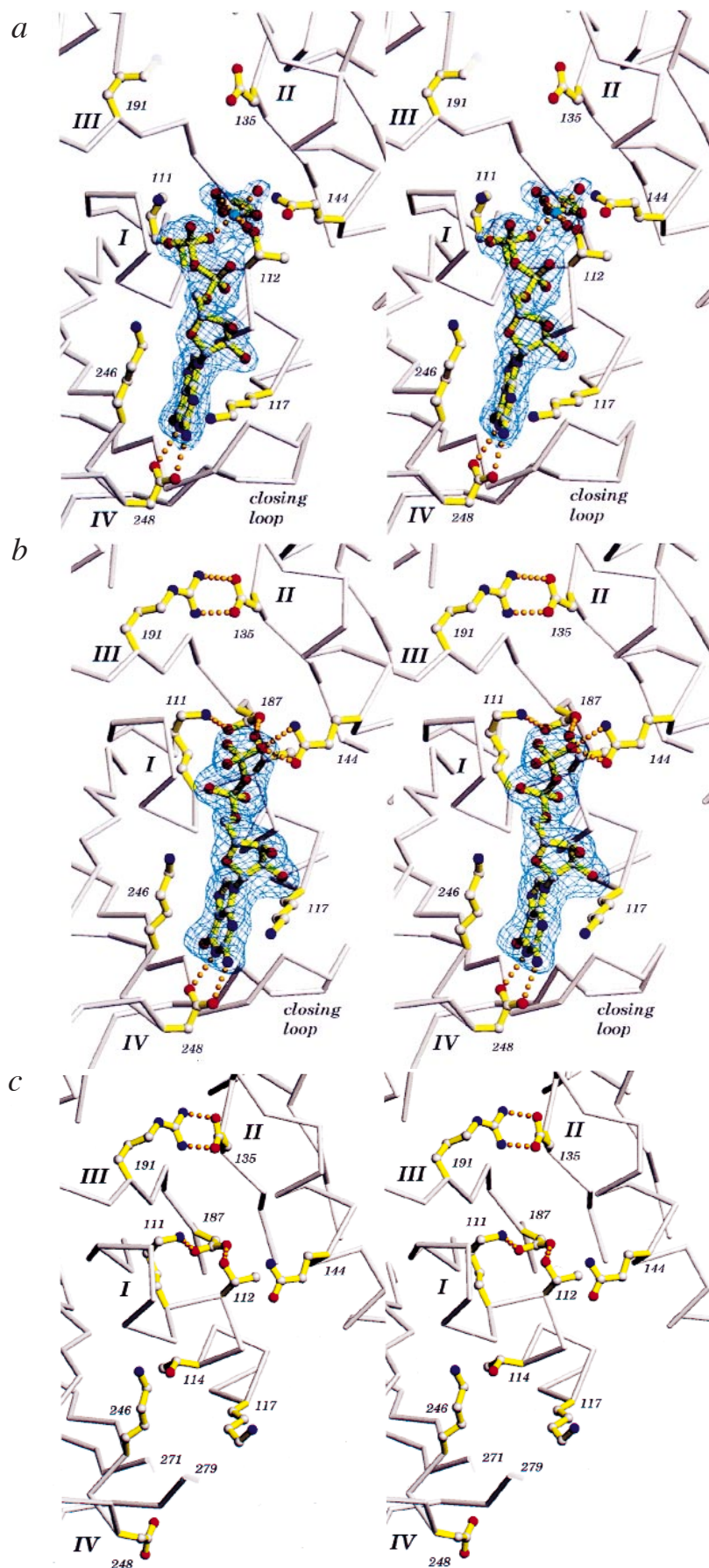


Fig. 2 The nucleotide-binding site in the GDP structures (G2 and G1), and the apo structure (A1). **a**, In the Mg^{2+} -GDP complex (G2) the β -phosphate is, typical of other GDP bound GTPase structures^{25–27}, curled under the P-loop. The magnesium ion is coordinated by the side chain hydroxyl of Thr 112, a phosphate oxygen and four water molecules. The salt bridges observed in the apo-NG active site are broken, so that Lys 111 turns toward the bound phosphate and the side chain of Arg 191 is disordered. **b**, In the magnesium-free GDP complex (G1) the β -phosphate is turned away from the P-loop, motif I, and interacts with highly conserved Gln 144, while the active site network of salt bridges is restored. **c**, In the apo structure (A1) (but not A2) the closing loop between residues 271 and 279 is disordered. The side chains of Thr 114, Lys 117, Lys 246 and Asp 248 each have roles in binding the guanine base, but have no specific interactions in its absence. Electron density maps were calculated with coefficients $(F_o - F_c)\phi_c$ after omitting the ligands, and are contoured at 3 σ .

and the extended side chain of Lys 246 of motif IV on the other (Fig. 3a).

In most GTPases the G-5 loop contributes a highly conserved hydrogen bond to the guanine O6 atom (see Fig. 3b). There is no such interaction between the guanine base and the closing loop of the SRP GTPase. Instead, the guanine O6 forms a hydrogen bond to the backbone amide of Lys 246, although the geometry and distance (3.14 Å) suggest that the interaction is relatively weak. The buried guanine N7, however, is hydrogen bonded to a solvent-inaccessible water that is positioned by interactions with the side chains of Lys 117 and Thr 114 (Fig. 3a). These residues, which originate from the α 1-helix, are uniquely conserved in the SRP GTPase subfamily (Fig. 1b) and contribute to a polar surface at the floor of the GTP-binding site that contrasts with the hydrophobic environment of the pocket seen in most other GTPases (Fig. 3b). The Lys side chain contributes two additional hydrogen bonds to the backbone carbonyl oxygens of closing loop residues Ser 273 and Gly 278. These serve to organize the base of the closing loop, so that two flexible elements, the Lys side chain and the closing loop, bridge the guanine nucleotide-binding site.

Coordination of the magnesium ion

The positions of the nucleotide phosphate groups and the octahedral coordination of the magnesium are well defined in the electron density map (Fig. 2a). The coordinating ligands for the Mg^{2+} ion are supplied by the O3 β -phosphate oxygen of the bound nucleotide, the side chain hydroxyl of motif I residue Thr 112, and four water molecules, and are typical of the coordination of Mg^{2+} -GDP seen in other GTPases^{25–27}. A secondary coordination sphere is contributed by oxygens of the α - and β -phosphates, three additional water molecules, and the side chains of Gln 144 and Asp 187.

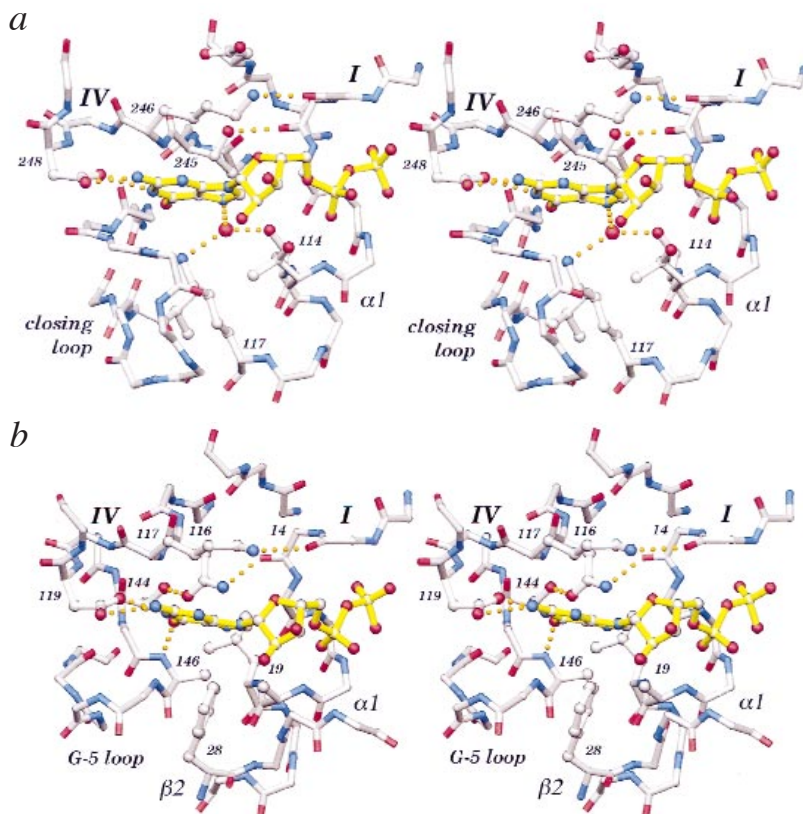


Fig. 3 Comparison of the GDP-binding interactions in Ffh (G2) with those in Ras (4q21). **a**, In Ffh, the 'closing loop' wraps around Lys 117 and forms van der Waals contacts with the guanine base. Lys 117 and Thr 114 are bridged by a buried water molecule that forms the floor of the binding site and provides a hydrogen bond to the guanine N7. Motifs I and IV are coupled by interactions of Lys 246 and Thr 245 with carbonyl oxygens of the motif I backbone. **b**, In Ras, Asn 116 bridges the binding site by hydrogen-bonding the carbonyl oxygen of motif I Val 14 and the hydroxyl of Thr 144 of the G-5 loop. The G-5 loop provides a hydrogen bond from Ala 146 to the guanine O6; similar O6 hydrogen bonding is present in other GTPases, but is absent in Ffh. The hydrophobic character of the floor of the binding site is also typical of most other GTPases (but not the Rho subfamily of GTPases, which includes buried water molecules^{46,47}). A packing interaction structurally analogous to the 'closing loop' in Ffh is provided by Phe 28 from the α 1-helix in Ras; in other GTPases, it is provided by elements of the Σ 4 loop.

Comparison with the apo structures reveals that the protein undergoes several small adjustments in this region on binding Mg^{2+} GDP. The β -phosphate is accommodated in the P-loop by small backbone shifts (~ 0.6 Å) that enable formation of several amide-phosphate hydrogen bonds and coordination of the magnesium by the side chain hydroxyl of Thr 112. The effect of these movements is a subtle opening of the motif I P-loop, resulting in both a small rotation of the α 1-helix and a small displacement at the beginning of motif I. In addition, recruitment of motif II Asp 187 to the magnesium site releases the salt bridge with Lys 111, allowing the Lys side chain to flip around and position its N ζ 3.15 Å from the β -phosphate oxygen (compare Fig. 2a and c). Finally, movement of the motif I main chain is coupled to movement of motif III by a hydrogen bond maintained between the amide nitrogen of Gln 107 and the carbonyl oxygen of Arg 191 (Fig. 4c).

Response of the motif II loop to Mg^{2+} nucleotide

These small shifts, and rearrangement of the water structure in the active site, contribute to the disruption of the salt bridge between motif III Arg 191 and motif II Asp 135 (Fig. 2a). Although there are small shifts in the motif III loop in each of the structures determined, in the Mg^{2+} GDP complex the disruption of these side chain interactions is accompanied by a significant and striking destabilization of the main chain atoms of the motif II loop. This is evidenced by elevated temperature factors throughout the motif II (Fig. 4a), and residues Thr 136–Pro 139, in particular, are located in very weak electron density. Thus, the network of side chain interactions observed in the apo-NG active site is completely disrupted by binding Mg^{2+} GDP, and binding interactions local to the P-loop destabilize main chain atoms 9–12 Å away. Strikingly, the disorder is local to the motif II loop; the remainder of the IBD (which comprises residues 128–181) remains essentially unchanged on binding Mg^{2+} GDP (Fig. 4b).

Interestingly, the conformation of the conserved Gly 190 of motif III is also directly affected by the disruption of the active site side chain interactions. This Gly is universally conserved in GTPases and appears to be critical for positioning the γ -phosphate of bound GTP. In the apo structures of the NG domain the carbonyl oxygen of Gly 190 is hydrogen bonded to the side chain of Arg 191 (Fig. 4c). In the Mg^{2+} GDP complex structure the hydrogen bond is disrupted as the side chain of Arg 191 becomes disordered. This frees the Gly residue and allows its oxygen and amide nitrogen atoms to orient toward the active site in a movement accompanied by a ~ 1.0 Å shift of the C α atoms of Gly 190 and Arg 191 (Fig. 4c).

The crystallization conditions and crystal packing interactions of the second apo-NG crystal form are identical to that of the Mg^{2+} GDP form. Nevertheless, in that structure the characteristic 'apo' active site side chain interactions are present and the residues of motif II are well defined in the electron density map. We conclude from this that the disruption of the network of active site side chain interactions observed in the Mg^{2+} GDP structure, and the corresponding disorder of the motifs II and III, are specific to the Mg^{2+} GDP-bound state.

The orientations of the N and G domains change

The structures of the apo and GDP complexes of the NG domain reveal two essentially rigid structural elements in the SRP GTPase. The first element comprises the α -helices of the N domain four-helix bundle (and the C-terminal helix that packs against it), which form a tightly packed hydrophobic core. The N domains of the different structures superimpose with root mean square (r.m.s.) shifts on C α atoms of ~ 0.4 Å between each pair. The second element is built around the β -sheet of the G domain and comprises the central β -sheet and the helices most distant from the N-domain that pack against it (the IBD, and helices α 1 and α 2). This core region of the G domain superim-

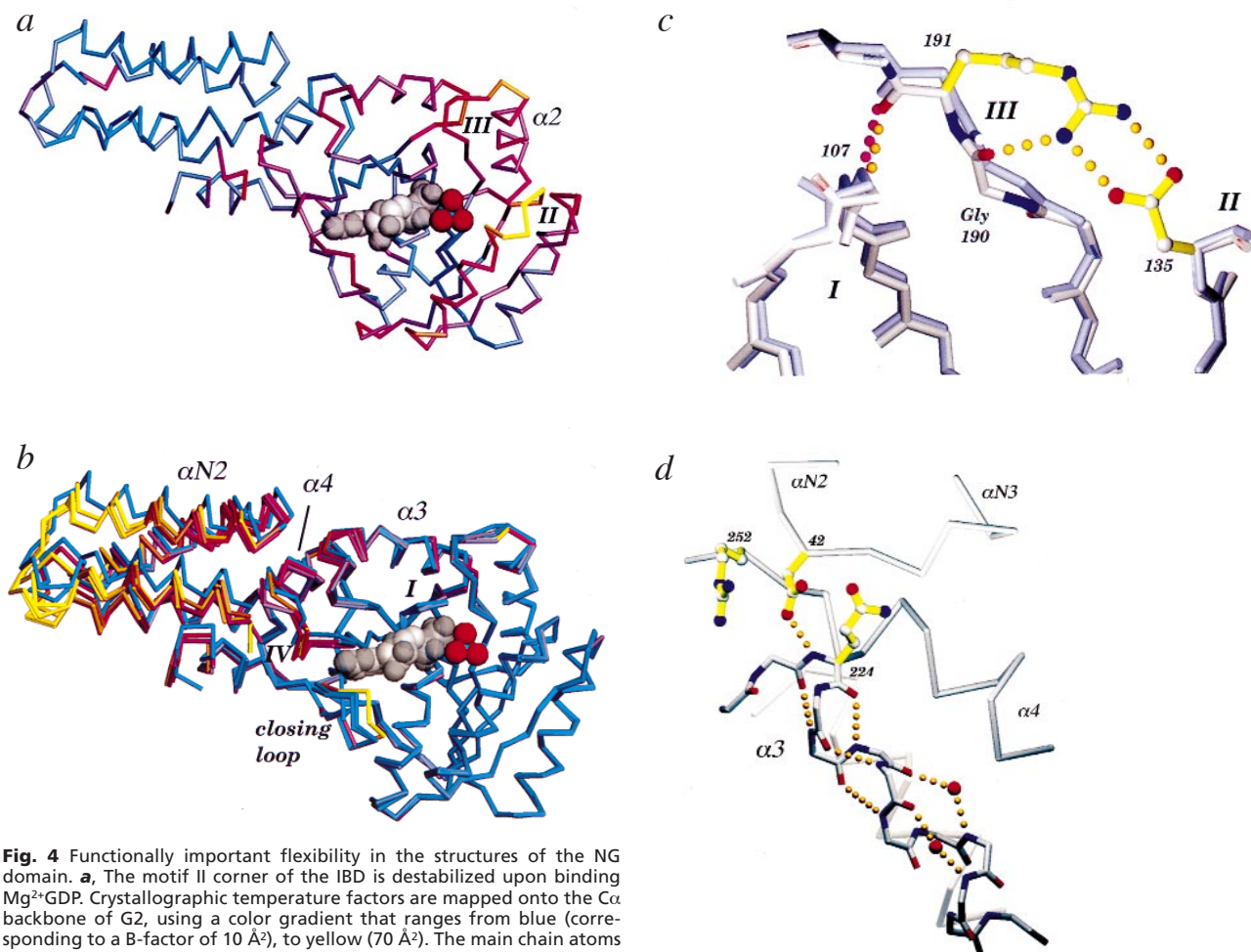


Fig. 4 Functionally important flexibility in the structures of the NG domain. **a**, The motif II corner of the IBD is destabilized upon binding $Mg^{2+}GDP$. Crystallographic temperature factors are mapped onto the α backbone of G2, using a color gradient that ranges from blue (corresponding to a B-factor of 10 \AA^2), to yellow (70 \AA^2). The main chain atoms of motif II (residues Thr 136–Ala 140) show substantial disorder, as do the amino-terminal residues of helix $\alpha 2$, which follow motif III. **b**, The interface between the N and G domains is flexible. The four structures of the Ffh NG (A1, G1, A2, G2) are superimposed over the core of the G domain. The magnitude of the shift relative to the apo (A1) structure is mapped onto the α backbone of each, using a color gradient that ranges from blue ($<0.01 \text{ \AA}$ shift) to yellow (2.5 \AA). Note that the G domain, particularly the 50 residues of the IBD (at right in the figure), is fairly rigid. The shift in position of the N domain accompanies movement of the motif IV and the ‘closing’ loops toward the bound nucleotide. **c**, Disruption of three hydrogen bonds of the Arg 191 side chain frees Gly 190 in the $Mg^{2+}GDP$ complex. Backbone atoms of motifs I, II and III in the apo and $Mg^{2+}GDP$ complex structures are superimposed, along with the hydrogen bonded conformation of the Arg 191 and Asp 135 side chains seen in the apo structure. The hydrogen bond (upper left) between main chain atoms of motifs I and III is maintained in each structure and may help position the two motifs. **d**, Transition of helix $\alpha 3$ between α - and 3_{10} -conformations. The main chain atoms of helix $\alpha 3$ in its ‘GDP’ $3_{10}/\alpha$ conformation are shown superimposed on a α diagram of the shorter ‘apo’ α -helical conformation. The N-terminal 3_{10} hydrogen bonding pattern is indicated, as are the two water molecules that interject into the helix. Several highly conserved side chains are shown; Asp 42 of the ALLEADV motif forms a hydrogen bond with the backbone amide of Gln 224.

poses with r.m.s. shifts on $C\alpha$ atoms of $\sim 0.3\text{--}0.5 \text{ \AA}$ between each pair of structures.

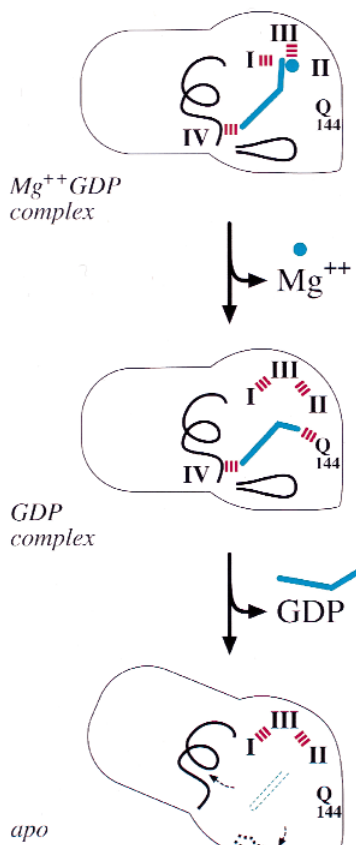
These two structural elements are connected across a highly conserved, flexible interface that allows the N and G domains to move during binding and release of nucleotide (Fig. 4b). The flexibility can be described as a rolling movement of the N domain, approximately along the axis of the helix $\alpha N4$, which, in the $Mg^{2+}GDP$ structure, translates the distal end of the N domain by $\sim 2.5 \text{ \AA}$ relative to its position in the apo structure A1 (Fig. 4b). The $\alpha 4$ - (DARGG-) helix of the G domain moves with the N domain so that the N-terminal end of the helix shifts by $\sim 1.5 \text{ \AA}$. A hydrophobic interface comprising highly conserved residues of the ALLEADV and DARGG motifs (Fig. 1b) serves as the ‘glue’ between the two domains. Water-mediated hydrogen bonds between the N-terminal end of the $\alpha 4$ -helix and Asp 250 couple the $\alpha 4$ -helix shift to a translation of the motif IV/DARGG loop

(residues Gly 249–Gly 253; Fig. 1b), resulting in movement of the side chain of motif IV Asp 248 $\sim 1.5 \text{ \AA}$ into the active site.

G domain helix $\alpha 3$ is adjacent to this domain interface and accommodates the structural flexibility between the N and G domains by switching to a 3_{10} -helical conformation halfway along its length in the nucleotide-bound state. This conversion lengthens the helix relative to the α -conformation observed in the apo (A1) structure (Fig. 4d) and allows the highly conserved $\alpha 3$ N-terminal residues Gly 223 and Gln 224 to move with the $\alpha 4$ -helix while the C-terminus of the helix remains fixed relative to the core β -sheet. The switch is aided by the interjection of two water molecules after residue Ser 228 and appears to be driven by the increased twist in the core β -sheet of the G domain and by a hydrogen bond maintained between the N-terminus of helix $\alpha 3$ and the highly conserved Asp 42 of the ALLEADV motif of the N domain. Several other conserved side chains located near the

articles

Fig. 5 Cartoon summarizing the structural consequences of binding of Mg^{2+} -GDP and GDP to NG. The three structures suggest a pathway for stepwise release of Mg^{2+} and GDP. GTPase sequence motifs I, II and III interact with the magnesium and phosphate groups. On release of Mg^{2+} (or perhaps $Mg^{2+}P_i$) they can form a network of hydrogen bonding interactions that stabilizes the nucleotide-free protein. Gln 144 is adjacent to the active site and can hydrogen bond the β -phosphate of the product GDP, thereby opening up the active site for product release. The closing loop, depicted at the bottom of the active site, packs against the bound nucleotide but on nucleotide release moves away and becomes disordered. The position of motif IV, which provides recognition of the guanine base, is coupled to the position of the N domain. The concerted action of the four elements presumably allows regulation of binding and release, and can explain the low nucleotide affinity of the SRP GTPase.



domain interface, including that of Arg 252 and Gln 224, do not appear to make specific interactions.

Structure of the GDP complex

The SRP GTPase can bind GDP in the absence of magnesium with only a relatively small change in binding affinity¹² (D.M.F., unpublished data). The structure of the magnesium-free GDP complex is similar to that of the Mg^{2+} -GDP complex, but not identical, as a small reorientation (~ 0.5 Å shift) of the GDP relative to its position in the Mg^{2+} -GDP complex is accommodated by looser packing of the closing loop against the guanine base. The most striking difference, however, is that the β -phosphate of the GDP does not interact with the motif I P-loop (Fig. 2b). Instead, the β -phosphate is positioned 4 Å from the P-loop by a $\sim 140^\circ$ rotation around the O5'-P α bond, and interacts with the side chain of Gln 144 extending from helix $\alpha 1a$ of the IBD. Both the phosphate group and the glutamine side chain are well defined in the electron density map, and the phosphate O3B oxygen clearly forms a hydrogen bond to the Gln side chain (Fig. 2b). A water molecule is located in the P-loop near the position that would otherwise be occupied by the β -phosphate. Remarkably, the network of active site side chain interactions characteristic of the apo-NG is maintained in the GDP complex (Fig. 2b).

Gln 144 is universally conserved in the SRP GTPase subfamily (Fig. 1b). In the Mg^{2+} -GDP complex Gln 144 is poorly defined in the electron density map but is in position to hydrogen bond to waters coordinating the magnesium ion. Its unique interaction

with the rotated β -phosphate in the absence of magnesium suggests that it may have an important role in nucleotide binding or exchange. We are aware of three other GTPase structures with GDP bound in the absence of magnesium²⁸⁻³⁰; none reveals the shift in the position of the β -phosphate group observed in this structure.

The apo-NG reveals intrinsic domain flexibility

The new apo structure also reveals an intrinsic flexibility of the N and G domain interface. In this structure the orientation between the N and G domains is more similar to that observed in the GDP and Mg^{2+} -GDP complexes than to the apo structure A1 (Fig. 4b), although the side chain of motif IV Asp 248 is still ~ 1 Å from a position in which it could contribute to the nucleotide-binding site. The closing loop is also visible and has a conformation close to that observed in the GDP-bound structure, G1 (Fig. 4b). The interface between the two domains is found in slightly different conformations in the structure of the apo intact Ffh (which includes the C-terminal M-domain³¹) as well. These observations suggest that different conformers can be trapped by crystal packing forces, and support the proposal that the structural relationship of the N and G domains of the SRP GTPase is dynamic.

Implications for nucleotide release

The three new structures of the NG GTPase can be interpreted as snapshots of hypothetical final stages in the GTPase cycle in which the GDP form lacking Mg^{2+} represents an intermediate in product release (Fig. 5). In this way they allow us to begin to address the mechanism of nucleotide release in structural terms. After hydrolysis of GTP, Ffh disengages from its receptor and exchanges GDP for GTP to initiate another round of targeting. Unlike many other GTPases that require a separate nucleotide exchange factor, the SRP GTPases have a low affinity for GDP *in vitro*. Moser *et al.*¹³ have suggested that the SRP GTPases possess an 'intrinsic exchange activity,' and propose that the IBD, which is unique to the SRP GTPases, provides this functionality. The structures described here, however, show that there is minimal structural rearrangement within the IBD on binding Mg^{2+} -GDP, and suggest that the IBD is unlikely to function as the primary exchange factor in the SRP GTPase. Rather, the structures identify at least four discrete structural features of the protein that together may contribute to nucleotide release. These include the active site side chain hydrogen bonding network, Gln 144, the closing loop, and the flexibility of the interface between the N and G domains.

The well-ordered interactions between the conserved active site side chains observed in the apo form of *T. aquaticus* Ffh appear to be unprecedented in the GTPase superfamily. Indeed many GTPases are unstable in the absence of nucleotide²⁴. The interactions involve universally conserved residues of motifs I, II and III, and so are likely to be functionally significant in the mechanism of the SRP subfamily of GTPases. These interactions could stabilize the apo form of the protein and therefore help to drive nucleotide exchange.

Likewise the conformation of the β -phosphate in the magnesium-free GDP complex is novel for GTPase structures. The Gln residue that interacts with the β -phosphate, Gln 144, is invariant in the SRP GTPase subfamily, and could play a key role in facilitating nucleotide release. Hydrolysis of GTP generates a phosphate molecule that must separate from the nucleoside diphosphate. In the complex of the GTPase G_{1c1} with GDP and P_i , the phosphate is accommodated by a 1.2–1.7 Å shift of the G_{1c1} switch II main chain (corresponding to motif III of the SRP

Table 1 Data collection and refinement statistics

	Mg ²⁺ GDP (G2)		GDP (G1)		apo (A2)	
	P4 ₃ 2 ₁ 2		C2		P2 ₁ 2 ₁ 2 ₁	
Space group	P4 ₃ 2 ₁ 2		C2		P2 ₁ 2 ₁ 2 ₁	
Unit cell (Å)	a = b = 100.07, c = 73.49		a = 110.42, b = 54.22, c = 58.46, β = 119.62°		a = 73.31, b = 99.01, c = 99.83	
Resolution (Å)	2.03		2.02		2.30	
R _{sym} (%) ^{1,2}	8.9	(39.6)	7.2	(28.4)	7.2	(41.7)
R _{meas} (%) ³	9.6	(42.5)	9.4	(34.5)	8.1	(46.9)
Completeness (%)	100.0	(100.0)	93.0	(92.8)	98.6	(98.6)
Redundancy	8.0	(7.8)	3.2	(2.9)	4.7	(4.6)
Average I/σ(I)	18.2	(4.7)	12.9	(3.6)	14.9	(3.3)
Number of reflections F > σ(F) (test set)	22,424 (1,838)		16,898 (1,320)		28,595 (2,319)	
R _{cryst} (%) ⁴	18.9	(24.2)	20.0	(30.9)	19.9	(26.2)
R _{free} (%) ⁴	25.0	(26.3)	29.1	(35.1)	22.5	(28.1)
No. of protein atoms	2,267		2,261		2,267	
No. of GDP atoms	28		28		–	
No. of water molecules	166		72		106	
Average B-factor (Å ²)						
N domain	20		52		32	
G domain	26		35		37	
GDP	27		29		–	
Water molecules	29		43		39	

¹Value in parentheses is in the high resolution bin.

²R_{sym} = $\sum |I_h - \langle I_h \rangle| / \sum I_h$, where $\langle I_h \rangle$ is the average intensity over symmetry equivalents.

³R_{meas} is the R_{sym} corrected for observation redundancy as described by Diederichs and Karplus⁴⁸.

⁴R_{cryst} = $\sum |F_o - F_c| / \sum F_o$. R_{free} was calculated for a test set of reflections (8%) omitted from the refinement.

GTPase, Fig. 1b), relative to its position in the presence of a GTP analog³². It appears that the protein adjusts to accommodate the released phosphate, presumably to shuttle it away from the active site during the catalytic cycle. The structure of the NG GTPase in complex with GDP suggests that the SRP GTPase accomplishes the same goal differently. Upon hydrolysis of GTP the protein could adjust its conformation to recapture the stable empty state while allowing the β-phosphate group of the product GDP to swing away toward conserved Gln 144, thus relieving the steric constraints by movement of the nucleotide phosphate rather than by rearrangement of the protein structure itself.

A third element, the closing loop, is flexible and may also contribute to nucleotide exchange. Studies of the *Mycoplasma mycoides* Ffh reveal that the closing loop is protected from proteolysis in the presence of nucleotide but is sensitive to cleavage, and presumably poorly ordered, in its absence³³. The structures described here reveal that the closing loop, which is disordered in the absence of nucleotide (A1), becomes 'latched' to the binding site by hydrogen-bonding to the highly conserved Lys 117 of the α1-helix in the presence of Mg²⁺GDP. The interaction between these structural elements may allow them to act as a 'gate' on the active site, promoting nucleotide exchange when open and providing binding interactions when closed.

The N and G domains interact across a conserved interface that allows the domains to move several angstroms relative to one another upon binding to GDP. The motion involves both longitudinal and transverse rotation of the N domain as well as translation of the tightly held DARGG- (α4-) helix (Fig. 4b). The latter is directly coupled to movement of the motif IV loop into the active site. This conformational change could provide a control point for nucleotide exchange, as restriction of movement of the N domain would clearly prevent the formation of the hydro-

gen bonds between Asp 248 and the guanine base. In this way the N/G interface could allow regulation of nucleotide exchange by prying open the active site ('guanine side first'^{34,35}), with the remaining elements acting to unlatch the binding site or stabilize the empty state in concert.

Signaling the nucleotide bound state

Many residues in the N/G interface are highly conserved in the SRP GTPases. The structural relationship between the two domains is critically important for function in protein targeting, as substitution of any of the hydrophobic residues in the ALLEADV motif has an effect on signal sequence binding²¹. The presence of additional conserved residues on the protein surface surrounding the domain interface (Fig. 1b) also hints at its functional importance; however, many of those conserved residues, including Asp 40, Arg 252 and Gln 224, reveal no specific or well-ordered interactions in the structures described here. Interestingly, in the crystal structure of the intact Ffh this region of the protein is close to one of the observed contacts between the NG and M domains³¹. Since this surface would be sensitive to the relative orientation of the N and G domains, it may be ideally suited to allow the nucleotide-bound state of the G domain to be regulated by, or be signaled to, the M domain of Ffh or another component of the SRP pathway, including the SRP RNA or the receptor, FtsY.

The regions corresponding to motifs II and III of various GTPases are typically disordered or highly mobile when GDP is bound but form a well-ordered structure in the GTP complex, the conformation of motif III being almost superimposable between different GTPases³². The position of the Gly residue of motif III appears to be critical for GTPase activity. In the apo- and GDP structures of the SRP GTPase, Gly 190 of motif III is

locked into an 'apo' conformation by a hydrogen bond with Arg 191 (Fig. 4d), but is released to orient toward the active site in the Mg²⁺GDP structure following disruption of the active site network. This suggests that, like the motif II and III side chains, Gly 190 is also sequestered from the active site in the apo-Ffh and is released to interact with nucleotide by a switch mechanism unique to the SRP GTPases.

Interestingly, it is also in precisely the region of motifs II and III that a comparison of the structures of the apo-G domains of Ffh and FtsY reveals substantial conformational difference. A solvent-exposed hydrophobic surface¹⁷ between motif I, the motif III loop, and helix $\alpha 3$ is preserved in each of the *T. aquaticus* NG structures and in the structure of *T. aquaticus* Ffh. Its collapse, seen in the structure of *Escherichia coli* FtsY, may well be an artifact due to the relative thermal instability of the *E. coli* protein in the absence of a binding partner. This would explain why the stable pattern of hydrogen bonding interactions between the conserved active site residues of the structures described here is not also found in the apo *E. coli* FtsY structure, and is consistent with a conformational freedom in that part of the protein.

Mobility of the motif II and III loops is reminiscent of the common mechanism by which GTPases utilize the conformational change of the motif III- $\alpha 2$ region to signal the 'active' GTP-bound state. The disorder observed in the SRP GTPase motif II and motif III loops triggered by binding to Mg²⁺GDP may therefore be characteristic of a common feature of GTPase mechanism^{26,32} and may reflect a (possibly transient) intermediate between the Mg²⁺GTP bound and empty states. This suggests that these residues, well ordered in the apo-protein, undergo a large conformational change on binding nucleoside triphosphate, and that this change is triggered by the disruption of the hydrogen bonding interactions between the residues of motifs I, II and III during accommodation of the Mg²⁺GTP in its binding site. These residues will then be freed to function in GTP hydrolysis and may communicate the GTP-bound state between the SRP and its receptor SR.

Methods

Crystallization. The NG domain fragment of *T. aquaticus* Ffh was purified as described¹⁷. Protein was concentrated to ~30 mg ml⁻¹ (~1 mM) in water using a Centricon 30 (Amicon). Concentrations were determined using the Bradford protein assay (Biorad) standardized by quantitative amino acid analysis. GDP (Boehringer) was repurified by anion exchange HPLC before use. For the Mg²⁺-free GDP complex (G1), GDP was added to the protein to give a final concentration of 2 mM GDP, and crystals were grown by sitting-drop vapor diffusion against a reservoir of 35% (v/v) dioxane. For the Mg²⁺GDP protein complex (G2), GDP was added to protein at 13 mg ml⁻¹ (~0.4 mM) to a final concentration of 1.2 mM; then 50 mM CdSO₄ was added to a final concentration of 5 mM. Crystals were obtained by sitting-drop vapor diffusion over 10% (w/v) PEG 8000, 0.1 M sodium cacodylate, pH 6.5, 0.2 M magnesium acetate. Crystals of the apo-protein (A2) were obtained under the same conditions, but omitting GDP.

Data collection. Data sets were obtained from single crystals mounted in rayon loops and frozen in a cold N₂ gas stream³⁶. A 20% (v/v) ethylene glycol cryoprotectant mother liquor was used for each crystal. Data from the GDP (G1) complex were measured using an RAXIS IV image plate system mounted on a Rigaku rotating-anode source with MSC mirrors. Data from the Mg²⁺GDP (G2) and apo (A2) crystal forms were measured at SSRL beamline 7-1 using a MAR 30 cm image plate. The cryoprotectant mother liquor

was supplemented with 2 mM GDP when mounting the G2 crystal form. Data sets were processed using DENZO and SCALEPACK³⁷ with no sigma cut-off (Table 1). The molecular packing of the G1 crystal form is closely related to that of the previously published apo-NG (also space group C2, but different crystallization conditions)¹⁷. The G2 and A2 crystals grow from essentially identical conditions but belong to different space groups with very similar molecular packing arrangements. Crystallographic four-fold symmetry in the G2 form corresponds to a pseudo-four-fold in the A2 form, which has two-fold noncrystallographic symmetry.

Structure solution and refinement. The published structure of the apo-NG (A1) (PDB accession number 1ffh)¹⁷ provided the initial model for molecular replacement solutions of the G1 and G2 crystal forms using AMORE³⁸. For the A2 crystal form (which has two monomers in the asymmetric unit) a model of the G2 structure without ligands was used, and yielded two distinct solutions. The models were subjected to cycles of positional and slow-cooling refinement using X-PLOR³⁹. The dimer in the asymmetric unit was refined using strict noncrystallographic symmetry (NCS) restraints. Electron density maps were calculated using X-PLOR and inspected using O (ref. 40). Initial (2F_o - F_c) ϕ _c maps calculated using the molecular replacement solutions clearly revealed the positions of active site ligands, water molecules, and the eight-residue 'closing loop' not located in the initial apo-NG (A1) crystal structure¹⁷. A bulk solvent correction⁴¹ allowed inclusion of all data from 20 Å to the high-resolution limit during refinement and map calculations. Refinement statistics are presented in Table 1. The structural models include residues 1–294 (A2, G2) and residues 2–294 (G1) of the *T. aquaticus* Ffh sequence. There are no Ramachandran outliers⁴², and the r.m.s. deviations from ideality are 0.011 Å, 0.013 Å and 0.019 Å for bond lengths, and 1.575°, 1.032° and 1.065° for bond angles, respectively, for the G1, G2 and A2 structures. During refinement the target bond length for oxygen atoms coordinating the Mg²⁺ in G2 was 2.06 Å (ref. 43), but the energy was set artificially low so that the distances were free to adjust. Several molecules of the cryoprotectant ethylene glycol were located in each of the structures. One cadmium ion per monomer could be clearly identified in the G2 and A2 crystals; it mediates a crystal packing interaction by coordinating side chain oxygens of two Glu residues from one monomer and a Glu and Asp residue from the other. Finally, in the A2 structure of the apo-protein a peak interpreted as sulfate was located bound at the motif I P-loop.

Analysis. The least-squares superpositions of the NG structures were calculated using LSQMAN⁴⁴. The overall best fits between the structures of the NG GTPase and the GTPases Ras and FtsY (PDB accession numbers 4q21 and 1fts, respectively) were determined using the 'BRute' option in that program. The least-squares superpositions of the conserved P-loop structure (residues 101–116 in *T. aquaticus* NG) were then readily obtained and formed the basis for the structural comparisons presented here. Figures were generated using SETOR⁴⁵ and O (ref. 40).

Coordinates. Atomic coordinates for the structures of *T. aquaticus* Ffh NG domain described in this paper have PDB accession codes 1NG1 (G2), 2NG1 (G1) and 3NG1 (A2).

Acknowledgments

We thank J. Richardson of Duke University for an illuminating discussion. This work was begun while D.M.F. was a postdoctoral fellow in the laboratories of P.W. and R.M.S. It was supported by grants to P.W. and R.M.S. from the NIH and by the Herb Boyer Fund and the Biotechnology Program of the University of California. It is based in part on research conducted at the Stanford Synchrotron Radiation Laboratory (SSRL), a facility funded by the Department of Energy, Office of Basic Energy Sciences. P.W. is an investigator in the Howard Hughes Medical Institute.

Received 15 January, 1999; accepted 8 April, 1999.

1. Walter, P. & Johnson, A.E. Signal sequence recognition and protein targeting to the endoplasmic reticulum membrane. *Annu. Rev. Cell Biol.* **10**, 87–119 (1994).
2. Miller, J.D., Bernstein, H.D. & Walter, P. Interaction of *E. coli* Ffh/4.5S ribonucleoprotein and FtsY mimics that of mammalian signal recognition particle and its receptor. *Nature* **367**, 657–659 (1994).
3. Kusters, R. *et al.* The functioning of the SRP receptor FtsY in protein-targeting in *E. coli* is correlated with its ability to bind and hydrolyse GTP. *FEBS Lett.* **372**, 253–258 (1995).
4. Powers, T. & Walter, P. Co-translational protein targeting catalyzed by the *Escherichia coli* signal recognition particle and its receptor. *EMBO J.* **16**, 4880–4886 (1997).
5. Powers, T. & Walter, P. Reciprocal stimulation of GTP hydrolysis by two directly interacting GTPases. *Science* **269**, 1422–1424 (1995).
6. Hauser, S., Bacher, G., Dobberstein, B. & Lütcke, H. A complex of the signal sequence binding protein and the SRP RNA promotes translocation of nascent proteins. *EMBO J.* **14**, 5485–5493 (1995).
7. Rapiejko, P.J. & Gilmore, R. Signal sequence recognition and targeting of ribosomes to the endoplasmic reticulum by the signal recognition particle do not require GTP. *Mol. Biol. Cell* **5**, 887–897 (1994).
8. Connolly, T. & Gillmore, R. The signal recognition particle receptor mediates the GTP-dependent displacement of SRP from the signal sequence of the nascent polypeptide. *Cell* **57**, 599–610 (1989).
9. Zopf, D., Bernstein, H., Johnson, A.E. & Walter, P. The methionine-rich domain of the 54 kD protein subunit of the signal recognition particle contains an RNA binding site and can be crosslinked to a signal sequence. *EMBO J.* **9**, 4511–4517 (1990).
10. Römisch, K., Webb, J., Lingelbäch, K., Gausepohl, H. & Dobberstein, B. The 54-kD protein of signal recognition particle contains a methionine-rich RNA binding domain. *J. Cell Biol.* **111**, 1793–1802 (1990).
11. Lütcke, H., High, S., Römisch, K., Ashford, A.J. & Dobberstein, B. The methionine-rich domain of the 54 kDa subunit of signal recognition particle is sufficient for the interaction with signal sequences. *EMBO J.* **11**, 1543–1551 (1992).
12. Jagath, J.R., Rodnina, M.V., Lentzen, G. & Wintermeyer, W. Interaction of guanine nucleotides with the signal recognition particle from *Escherichia coli*. *Biochemistry* **37**, 15408–15413 (1998).
13. Moser, C., Mol, O., Goody, R.S. & Sinning, I. The signal recognition particle receptor of *Escherichia coli* (FtsY) has a nucleotide exchange factor built into the GTPase domain. *Proc. Natl. Acad. Sci. USA* **94**, 11339–11344 (1997).
14. Bacher, G., Lütcke, H., Jungnickel, B., Rapoport, T.A. & Dobberstein, B. Regulation by the ribosome of the GTPase of the signal-recognition particle during protein targeting. *Nature* **381**, 248–251 (1996).
15. Miller, J.D., Wilhelm, H., Gierasch, L., Gilmore, R. & Walter, P. GTP binding and hydrolysis by the signal recognition particle during initiation of protein translocation. *Nature* **366**, 351–354 (1993).
16. Rapiejko, P.J. & Gilmore, R. Empty site forms of the SRP54 and SR alpha GTPases mediate targeting of ribosome-nascent chain complexes to the endoplasmic reticulum. *Cell* **89**, 703–713 (1997).
17. Freymann, D.M., Keenan, R.J., Stroud, R.M. & Walter, P. Structure of the conserved GTPase domain of the signal recognition particle. *Nature* **385**, 361–364 (1997).
18. Montoya, G., Svensson, C., Lührink, J. & Sinning, I. Crystal structure of the NG domain from the signal-recognition particle receptor FtsY. *Nature* **385**, 365–369 (1997).
19. Zheng, N. & Gierasch, L.M. Domain interactions in *E. coli* SRP: stabilization of M domain by RNA is required for effective signal sequence modulation of NG domain. *Mol. Cell* **1**, 1–20 (1997).
20. Zopf, D., Bernstein, H.D. & Walter, P. GTPase domain of the 54-kD subunit of the mammalian signal recognition particle is required for protein translocation but not for signal sequence binding. *J. Cell Biol.* **120**, 1113–1121 (1993).
21. Newitt, J.A. & Bernstein, H.D. The N-domain of the signal recognition particle 54-kDa subunit promotes efficient signal sequence binding. *Eur. J. Biochem.* **245**, 720–729 (1997).
22. Bourne, H.R., Sanders, D.A. & McCormick, F. The GTPase superfamily: a conserved switch for diverse cell functions. *Nature* **348**, 125–132 (1990).
23. Kjeldgaard, M., Nyborg, J. & Clark, B.F.C. The GTP binding motif: variations on a theme. *FASEB J.* **10**, 1347–1368 (1996).
24. Sprang, S.R. G Protein mechanisms: insights from structural analysis. *Annu. Rev. Biochem.* **66**, 639–678 (1997).
25. Kjeldgaard, M. & Nyborg, J. Refined structure of elongation factor Tu from *Escherichia coli*. *J. Mol. Biol.* **223**, 721–742 (1992).
26. Tong, L.A., de Vos, A.M., Milburn, M.V. & Kim, S.H. Crystal structures at 2.2 Å resolution of the catalytic domains of normal ras protein and an oncogenic mutant complexed with GDP. *J. Mol. Biol.* **217**, 503–516 (1991).
27. Scheffzek, K., Klebe, C., Fritz-Wolf, K., Kabsch, W. & Wittinghofer, A. Crystal structure of the nuclear Ras-related protein Ran in its GDP-bound form. *Nature* **374**, 378–381 (1995).
28. Al-Karadaghi, S., Åvarsson, A., Garber, M., Zheltonosova, J. & Liljas, A. The structure of the elongation factor G in complex with GDP: conformational flexibility and nucleotide exchange. *Structure* **4**, 555–565 (1996).
29. Czworkowski, J., Wang, J., Steitz, T.A. & Moore, P.B. The crystal structure of elongation factor G complexed with GDP, at 2.7 Å resolution. *EMBO J.* **13**, 3661–3668 (1994).
30. Mixon, M.B. *et al.* Tertiary and quaternary structural changes in G_{10i1} induced by GTP hydrolysis. *Science* **270**, 954–960 (1995).
31. Keenan, R.J., Freymann, D.M., Walter, P. & Stroud, R.M. Crystal structure of the signal sequence binding subunit of the signal recognition particle. *Cell* **94**, 181–191 (1998).
32. Berghuis, A.M., Lee, E., Raw, A.S., Gilman, A.G. & Sprang, S.R. Structure of the GDP-P_i complex of Gly203→Ala Gα1: a mimic of the ternary product complex of Gα-catalyzed GTP hydrolysis. *Structure* **4**, 1277–1290 (1996).
33. Indery, M., Macao, B., Larsson, T. & Samuelsson, T. Binding of GTP and GDP induces a significant conformational change in the GTPase domain of Ffh, a bacterial homologue of the SRP 54 kDa subunit. *Biochim. Biophys. Acta* **1385**, 61–68 (1998).
34. Böhm, A., Gaudet, R. & Sigler, P.B. Structural aspects of heterotrimeric G-protein signaling. *Curr. Opin. Biotechnol.* **8**, 480–487 (1997).
35. Onrust, R. *et al.* Receptor and betagamma binding sites in the alpha subunit of the retinal G protein transducin. *Science* **275**, 381–384 (1997).
36. Teng, T.-Y. Mounting of crystals for macromolecular crystallography in a free-standing thin film. *J. Appl. Crystallogr.* **23**, 387–391 (1990).
37. Otwinowski, Z. Oscillation data reduction program. In *Data collection and processing* (eds Sawyer, L., Isaacs, N.W. & Bailey, S.) 55–62 (SERC Daresbury Laboratory, Warrington, United Kingdom; 1993).
38. Navaza, J. AMoRe: an automated package for molecular replacement. *Acta Crystallogr. A* **50**, 157–163 (1994).
39. Brünger, A.T. *X-PLOR: a system for X-ray crystallography and NMR*. (Yale University Press, New Haven, Connecticut; 1992).
40. Jones, T.A., Zou, J.Y., Cowan, S.W. & Kjeldgaard, M. Improved methods for building protein models in electron density maps and the location of errors in these models. *Acta Crystallogr. A* **47**, 110–119 (1991).
41. Jiang, J.-S. & Brünger, A.T. Protein hydration observed by X-ray diffraction. *J. Mol. Biol.* **243**, 100–115 (1994).
42. Laskowski, R.A., MacArthur, M.W., Moss, D.S. & Thornton, J.M. PROCHECK: a program to check the stereochemical quality of protein structures. *J. Appl. Crystallogr.* **26**, 283–291 (1993).
43. Glusker, J.P. Structural aspects of metal liganding to functional groups of proteins. *Adv. Protein Chem.* **42**, 1–76 (1991).
44. Kleywegt, G.J. & Jones, T.A. Detecting folding motifs and similarities in protein structures. *Methods Enzymol.* **277**, 525–545 (1997).
45. Evans, S.V. SETOR: hardware-lighted three-dimensional solid model representations of macromolecules. *J. Mol. Graph.* **11**, 134–138 (1993).
46. Ihara, K. *et al.* Crystal structure of human RhoA in a dominantly active form complexed with a GTP analogue. *J. Biol. Chem.* **273**, 9656–9666 (1998).
47. Hirschberg, M., Stockley, R.W., Dodson, G. & Webb, M.R. The crystal structure of human rac1, a member of the Rho family complexed with a GTP analogue. *Nature Struct. Biol.* **4**, 147–151 (1997).
48. Diederichs, K. & Karplus, P.A. Improved R-factors for diffraction data analysis in macromolecular crystallography. *Nature Struct. Biol.* **4**, 269–275 (1997).